





Effect of Neutron Irradiation on the Structure and Atomic Dynamics of Y_2O_3 Nanoparticles

J.I. Huseynov*, A.O. Dashdamirov , R.F. Rzayev ,
G.A. Aslanov

Azerbaijan State Pedagogical University, Baku, Azerbaijan
jahangirhuseynov1958@gmail.com

Abstract. This work investigates the structural stability and atomic dynamics of high-purity Y_2O_3 nanoparticles under neutron irradiation. Experimental studies were carried out using scanning electron microscopy (SEM), X-ray diffraction (XRD), and Raman spectroscopy. For the high symmetry cubic phase (space group Ia-3), the lattice parameters and interatomic distances were determined. It was found that upon neutron irradiation with varying intensities (4.0×10^{12} – 10^{15} n/cm²), the main symmetry of the crystalline structure is preserved and no new phases are formed. Raman spectra analysis revealed no significant changes in the frequencies of the main vibrational modes observed at 1081 and 1531 cm⁻¹. However, at high irradiation doses, an increase in the background level was detected, which is attributed to partial amorphization of the structure. The obtained results indicate the high radiation resistance of Y_2O_3 nanoparticles, making them promising materials for applications in optoelectronics and nuclear technologies.

Keywords: Y_2O_3 nanoparticles, neutron irradiation, Raman spectroscopy, X-ray diffraction, crystal structure, radiation resistance.

1 Introduction

Yttrium oxide Y_2O_3 is a high-quality ceramic material distinguished by its excellent corrosion resistance, chemical and thermal stability, high melting point, low thermal expansion coefficient, and high thermal conductivity. Y_2O_3 nanoparticles (Y_2O_3 NPs) are widely used in various fields of modern materials science and technology due to their unique physical, chemical, and optical properties. Owing to their pronounced fluorescence properties, Y_2O_3 nanoparticles are employed as phosphors. When doped with rare-earth elements (e.g., Er, Eu, Tb), they exhibit the ability to convert infrared radiation into the

visible region of the spectrum, making them promising for use in laser systems, display technologies, and light-emitting diodes [1–3]. The material is characterized by broad transparency in the spectral range of 0.2–8 μm , a high dielectric constant (~ 14 – 18), a large refractive index (~ 2), and a wide band gap (~ 5.8 eV). These outstanding electronic characteristics make Y_2O_3 of particular interest to researchers developing efficient optoelectronic devices [4]. The high thermal and chemical stability of Y_2O_3 nanoparticles also contributes to their use in heterogeneous catalysis. They serve as catalysts or catalyst supports in reactions such as methane steam reforming, CO oxidation, and NO_x reduction. Y_2O_3 nanoparticles exhibit antioxidant and radioprotective properties, as well as antitumor activity and potential use as drug carriers [5].

Their biocompatibility and low toxicity make this material promising for biomedical imaging and therapy.

2 Research Methodology

The object of the study was Y_2O_3 nanocrystals with a density of 0.31 g/cm³, a purity of 99.995%, crystalline particle sizes ranging from 30 to 45 nm, a specific surface area (SSA) of 25–45 m²/g, a melting temperature of 2425 °C, and an evaporation temperature of 4300 °C.

In studying the structural properties of Y_2O_3 nanoparticles, particular attention was paid to their surface structure and size effect. The experiments were carried out using a ZEISS IGMA VP scanning electron microscope under conditions that minimized external influences. The structural characteristics of the samples were determined by X-ray diffraction using a D8 Advance diffractometer, while the atomic dynamics were examined by Raman spectroscopy at room temperature and under normal conditions. The obtained results were analyzed using the Rietveld method with the FullProf program and further approximated by Gaussian functions using Origin software.

During the experiments, an Nd:YAG laser with a wavelength of 532 nm and a maximum power of 10 mW was used as the excitation source in the Raman spectrometer. Raman spectra analysis was performed in Origin 9 by determining the positions of maxima approximated by Gaussian functions, which made it possible to identify the features of atomic dynamics in the studied material.

Irradiation of yttrium oxide nanoparticles with high-intensity neutrons of energy $E < 1$ MeV was carried out at the IBR-2 research reactor (Joint Institute for Nuclear Research, Dubna, Russia) at five different intensities [10]:

$$I = 4.0 \times 10^{12}, 8.0 \times 10^{12}, 1.3 \times 10^{13}, 4.0 \times 10^{14}, 1.0 \times 10^{15} \text{ n/cm}^2.$$

After irradiation, the activity of the samples was monitored. The investigation

of the crystalline structure of yttrium oxide nanoparticles by X-ray diffraction (XRD) at room temperature revealed that the Y_2O_3 compound possesses high symmetry. The unit cell corresponds to a cubic syngony with a space group of $Ia\bar{3}$. The unit cell parameters are $a = b = c = 10.5958 \text{ \AA}$. It is known that the oxidation state of yttrium is +3. Rietveld refinement analysis showed that trivalent yttrium atoms occupy two different crystallographic positions in the crystal lattice. The first yttrium atom (Y1) is located at coordinates $x = 0.25, y = 0.25, z = 0.25$, while the second yttrium atom (Y2) is positioned at $x = -0.0165, y = 0, z = 0.25$. Divalent oxygen atoms occupy identical crystallographic positions: $x = 0.3942, y = 0.1428, z = 0.3825$.

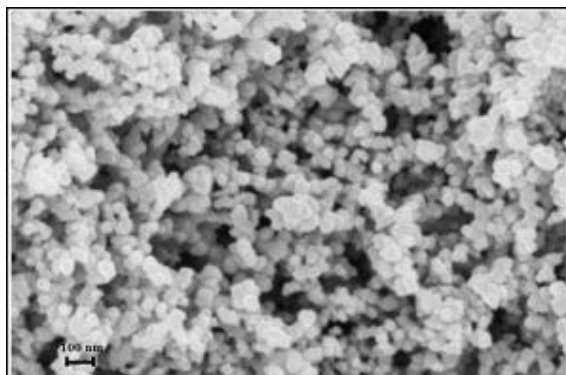


Fig. 1. Surface morphology of Y_2O_3 nanoparticles

Oxygen atoms form covalent bonds with yttrium atoms of varying lengths in the range of $d(O - Y) = 2.1628\text{--}2.4083 \text{ \AA}$. The bond lengths between identical atoms are slightly larger. Analysis of the crystal structure using the Diamond 3.2 software showed that the distances between the nearest oxygen atoms are $d(O - O) = 2.8207\text{--}3.7003 \text{ \AA}$, while those between the nearest yttrium atoms are $d(Y - Y) = 3.6416\text{--}3.8922 \text{ \AA}$. A comparison of interatomic distances indicates that as the ionic radii increase, atoms are positioned farther apart. Consequently, slight variations in bond lengths are observed. Oxygen atoms, being light elements, have smaller ionic radii, whereas yttrium atoms, belonging to the rare-earth elements, possess larger radii. During covalent bond formation, yttrium electrons fill the outer electron shell of oxygen atoms, resulting in an increase in the ionic radius of divalent oxygen atoms. This explains why O–O bond lengths exceed those of O–Y bonds.

The analysis of X-ray diffraction patterns Figure 2 of Y_2O_3 nanoparticles exposed to neutron irradiation of varying intensities showed that no significant changes occur in their crystalline structure. According to Rietveld refinement results, all samples exhibit cubic symmetry with a space group of $Ia\bar{3}$, and the

diffraction peaks of the non-irradiated sample are also observed in the samples irradiated at intensities up to

10^{15} n/cm². This indicates that under ionizing radiation, no new phase is formed and the crystalline structure remains stable.

With increasing irradiation intensity, three main effects were observed:

1) a shift of diffraction peaks toward larger angles (associated with an increase in interatomic distances and lattice parameters), 2) a decrease in peak intensities (while maintaining the relative atomic positions), and

3) an increase in background level (caused by partial amorphization). In general, it was established that under neutron irradiation with energy $E < 1$ MeV and intensity up to 10^{15} n/cm², Y₂O₃ nanoparticles exhibit high radiation resistance and retain their highly symmetric crystalline structure.

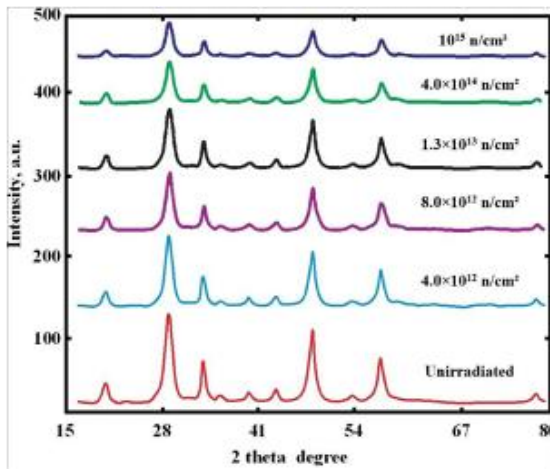


Fig. 2. X-ray diffraction spectra of Y₂O₃ nanoparticles irradiated at different intensities.

The Raman spectra of Y₂O₃ nanoparticles obtained at room temperature are shown in Figure 3. Raman spectroscopy does not allow the observation of all possible vibrational frequencies. In compounds with a highly symmetric crystal lattice, a smaller number of vibrational modes are observed. Since the crystal structure of Y₂O₃ nanoparticles corresponds to cubic symmetry with the space group Ia-3, only a limited number of vibrational modes are expected to be detected. According to Raman spectroscopy principles, vibrational frequencies of bonds formed by heavy atoms have lower values, while higher frequencies correspond to bonds formed by light atoms such as O, H, C, etc. As the atomic dynamics of Y₂O₃ nanoparticles are mainly associated with vibrations of oxygen atoms, the studies

were carried out in the high-frequency region, from 500 to 3000 cm^{-1} . Analysis of the Raman spectrum using Gaussian fitting revealed two vibrational modes in this frequency range. These modes, shown in Figure 4, were interpreted using Gaussian fitting performed in Origin 9 software. The spectrum shows that the lattice vibrations observed in yttrium oxide nanoparticles correspond to frequencies of 1081 cm^{-1} and 1531 cm^{-1} .

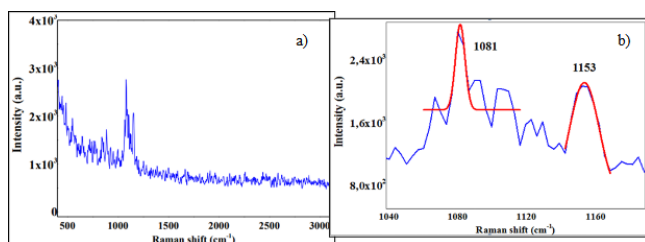


Fig. 3. Raman spectra of Y_2O_3 nanoparticles.

The high values of these Raman mode frequencies indicate that these vibrations correspond to Y–O bonds.

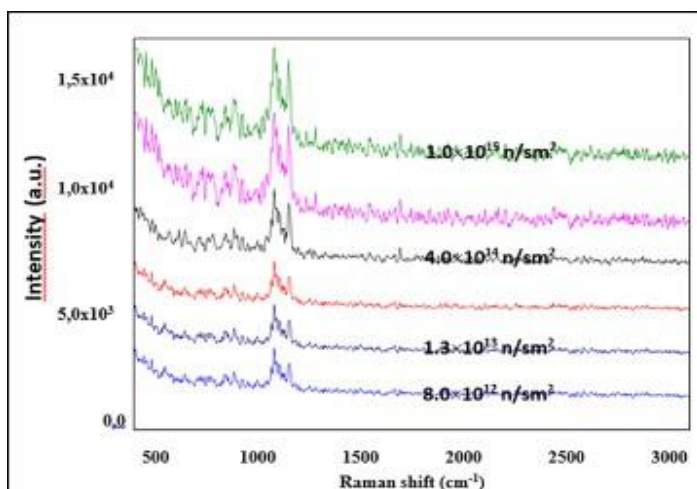


Fig. 4. Raman spectra of nano-sized Y_2O_3 samples irradiated with neutrons.

To study the changes under neutron irradiation, the atomic dynamics of samples exposed to high-intensity neutron fluxes were investigated.

Figure 5 presents the Raman spectra of nanosized Y_2O_3 samples irradiated with fast neutrons at various intensities up to 1.0×10^{15} n/cm^2 at room temperature. When comparing the Raman spectra of unirradiated and fast-

neutron irradiated Y_2O_3 nanoparticles, the same modes are observed in all cases. As irradiation intensity increases, an additional background appears in the spectra, associated with breaking weak bonds under the neutron flux, leading to partial disruption of the ideal structure and partial amorphization.

A detailed analysis of a sample irradiated at $I = 1.0 \times 10^{15}$ n/cm² using Gaussian fitting revealed two vibrational modes at 1081 cm⁻¹ and 1153 cm⁻¹, consistent with the unirradiated sample. This indicates that neutron irradiation does not cause significant changes in atomic dynamics.

The absence of changes in the frequencies of the observed vibrational modes confirms that bond lengths between yttrium and oxygen atoms remain unchanged. Although the Raman spectra show no major changes, the effect of high-energy neutrons is seen as an increase in background, corresponding to partial amorphization caused by breaking weak bonds. Thus, Raman spectroscopy confirms that nanostructured Y_2O_3 is a stable material with respect to external influences. This stability arises from nanoscale effects, high crystal symmetry, and strong lattice bonding, although partial structural changes can occur under fast neutron irradiation.

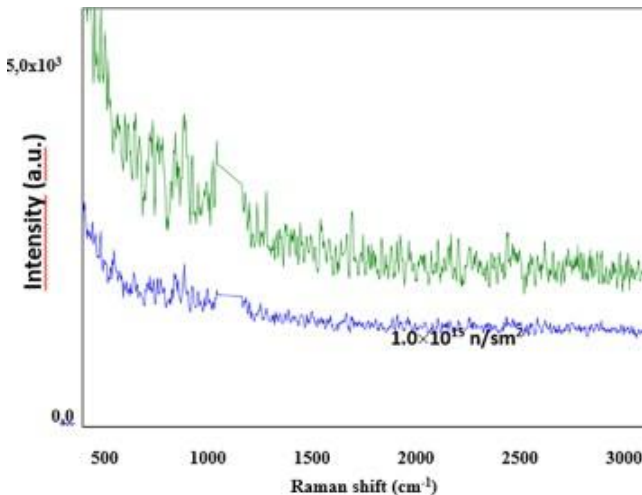


Fig. 5. Background of the Raman spectra of non-irradiated and neutron-irradiated (at an intensity of 10^{15} n/cm²) nano-sized Y_2O_3 compounds.

3 Conclusion

The conducted studies demonstrated that Y_2O_3 nanoparticles have sizes in the range of 20–40 nm and exhibit a homogeneous granular surface morphology.

According to X-ray diffraction data, Y_2O_3 crystallizes in a highly symmetric cubic structure (space group Ia-3). The lattice parameters were determined as $a = b = c = 10.5958 \text{ \AA}$. The crystallographic positions of atoms and interatomic distances were calculated, showing that increasing the neutron irradiation intensity up to 10^{15} n/cm^2 does not lead to significant changes in the crystal phase symmetry or lattice parameters. A slight shift of diffraction peaks toward higher angles and a partial reduction in their intensity is associated with minor variations in interatomic distances; however, this does not result in the formation of new phases. Overall, the results indicate that Y_2O_3 nanoparticles possess high radiation resistance and retain their crystalline structure. Raman spectroscopy results confirmed the stability of the atomic dynamics in Y_2O_3 nanoparticles. The main Raman modes observed in unirradiated samples correspond to frequencies of 1081 and 1531 cm^{-1} , characterizing the vibrational frequencies of Y-O bonds. Upon neutron irradiation at various intensities $4.0 \times 10^{12} - 10^{15} \text{ n/cm}^2$, no significant changes in the Raman mode frequencies were detected, indicating the preservation of Y-O bond lengths. An increase in the background level in the spectra at high irradiation intensity is explained by partial amorphization caused by local structural disruptions due to the breaking of weak chemical bonds. The analysis of the Raman spectra ultimately confirmed that Y_2O_3 nanoparticles demonstrate high radiation resistance even under exposure to external ionizing radiation, making them promising materials for applications in optoelectronics, nuclear technologies, and high temperature ceramic systems.

References

1. F. Vetrone, J.-C. Boyer, J. A. Capobianco, A. Speghini, M. Bettinelli, "Concentration-Dependent Near-Infrared to Visible Upconversion in Nanocrystalline and Bulk $\text{Y}_2\text{O}_3:\text{Er}^{3+}$," *Chemistry of Materials*, 15(14), 2737-2743, 2003.
2. M. M. Arghavan, A. A. Sabouri-Dodaran, M. Sasani Ghamsari, "Efficient route for preparation of Nd^{3+} doped Y_2O_3 nanoparticles at intermediate temperature," *Heliyon*, 10(4): e25864, 2024.
3. J. Dhanaraj, R. Jagannathan, T. R. N. Kutty, C.-H. Lu, "Photoluminescence Characteristics of $\text{Y}_2\text{O}_3:\text{Eu}^{3+}$ Nanophosphors Prepared Using Sol-Gel Thermolysis," *The Journal of Physical Chemistry B*, 105(45), 11098-11105, 2001.
4. C. V. Ramana, V. H. Mudavakkat, K. K. Bharathi, V. V. Atuchin, L. D. Pokrovsky, V. N. Kruchinin, "Enhanced optical constants of nanocrystalline yttrium oxide thin films," *Appl. Phys. Lett.*, 98, 031905, 2011.
5. N. Koslowski, R. C. Hoffmann, V. Trouillet, M. Bruns, S. Foroc, J. J. Schneider, "Synthesis, oxide formation, properties and thin film transistor properties of yttrium and aluminium oxide thin films employing a molecular-based precursor route," *RSC Adv.*, 9, 31386, 2019.

6. A. E. Nabiyev, J. I. Huseynov, “Growth of synthetic diamond films and their electrophysical properties,” *UNEC Journal of Engineering and Applied Sciences SECTION PHYSICS*, 3(2), 76–85, 2023.
7. G. Rajakumar, L. Mao, T. Bao et al., “Yttrium Oxide Nanoparticle Synthesis: An Overview of Methods of Preparation and Biomedical Applications,” *Appl. Sci.*, 11(5), 2172, 2021.
8. A. E. Nabiyev, J. I. Huseynov, I. I. Abbasov, “Dielectric properties of $\text{Ba}_{0.8}\text{Sr}_{0.2}\text{TiO}_3$ ferroelectric films in an alternating electric field,” *Canadian Journal of Physics*, 102(6), 325–331, 2024.
9. R. F. Rzayev, “Influence of neutron flux on the crystal structure of Y_2O_3 nanoparticles,” *Advanced Physical Research*, 4(2), 106–110, 2022.
10. A. O. Dashdemirov, J. I. Huseynov, R. F. Rzayev, Y. I. Aliyev, “Thermophysical behavior in Y_2O_3 under high intensity fast neutron irradiation,” *Modern Physics Letters B*, 36(20), 2022.

Open Access This chapter is licensed under the terms of the Creative Commons Attribution-NonCommercial 4.0 International License (<http://creativecommons.org/licenses/by-nc/4.0/>), which permits any noncommercial use, sharing, adaptation, distribution and reproduction in any medium or format, as long as you give appropriate credit to the original author(s) and the source, provide a link to the Creative Commons license and indicate if changes were made.

The images or other third party material in this chapter are included in the chapter's Creative Commons license, unless indicated otherwise in a credit line to the material. If material is not included in the chapter's Creative Commons license and your intended use is not permitted by statutory regulation or exceeds the permitted use, you will need to obtain permission directly from the copyright holder.

